Atmos. Chem. Phys. Discuss., 15, 29497–29521, 2015
www.atmos-chem-phys-discuss.net/15/29497/2015/
doi:10.5194/acpd-15-29497-2015

Atmospheric Chemistry and Physics Discussions

Upper-tropospheric humidity changes under constant relative humidity

K. Gierens[1] **and K. Eleftheratos**[2]

[1]Deutsches Zentrum für Luft- und Raumfahrt, Institut für Physik der Atmosphäre, Oberpfaffenhofen, Germany
[2]Faculty of Geology and Geoenvironment, University of Athens, Athens, Greece

Received: 15 September 2015 – Accepted: 14 October 2015 – Published: 29 October 2015

Correspondence to: K. Gierens (klaus.gierens@dlr.de)

Published by Copernicus Publications on behalf of the European Geosciences Union.

Abstract

Theoretical derivations are given on the change of upper-tropospheric humidity (UTH) in a warming climate. Considered view is that the atmosphere, getting moister with increasing temperatures, will retain a constant relative humidity. In the present study we show that the upper-tropospheric humidity, a weighted mean over a relative humidity profile, will change in spite of constant relative humidity. The simple reason for this is that the weighting function, that defines UTH, changes in a moister atmosphere. Through analytical calculations using observations and through radiative transfer calculations we demonstrate that two quantities that define the weighting function of UTH can change: the water vapour scale height and the peak emission altitude. Applying these changes to real profiles of relative humidity shows that absolute UTH changes typically do not exceed 1 %. If larger changes would be observed they would be an indication of climatological changes of relative humidity. As such, an increase in UTH between 1980 and 2009 in the northern midlatitudes as shown by earlier studies using HIRS data, may be an indication of an increase in relative humidity as well.

1 Introduction

Water vapour plays several distinct roles in the atmosphere. In the lower troposphere it is particularly relevant for weather whereas it is particularly relevant for climate in the upper troposphere and the stratosphere (Kiemle et al., 2012). The relevance for climate originates from the peculiar molecular line spectrum of the H_2O molecule. It has strong spectral lines at wavelengths exceeding 16 µm (rotation band) and at 6.3 µm (vibration-rotation band). These get optically thick in the upper troposphere and the stratosphere, that is, a satellite instrument that observes the Earth in these wavelength bands cannot look deeper into the atmosphere than into these emitting layers. Radiation from further below gets absorbed before it can leave the atmosphere. Although the amount of water vapour in these layers is only a small fraction of its total amount in the at-

ACPD
15, 29497–29521, 2015

mosphere the contribution of upper tropospheric humidity (UTH) to radiative cooling of the atmosphere is disproportionately large (Clough et al., 1992). In total, water vapour contributes 2/3 of the natural greenhouse effect.

There is a long-standing debate on the role of upper-tropospheric water vapour in a changing climate, i.e. under conditions where the troposphere gets warmer. Möller (1963) computed the change of surface temperature required to restore the net longwave radiation at the ground following an increase of the atmospheric CO_2 content. He assumed a fixed relative humidity which implies an increase of water vapour amount in all atmospheric levels where the temperature increases. His results suggested that the increase of water vapour amount with increasing temperature causes a self-amplification effect, i.e. he found that water vapour is able to feed into a positive greenhouse feedback loop. Some years later Manabe and Wetherald (1967) envisaged a world with constant relative humidity in their radiation-convection model and found that CO_2 doubling led to a surface temperature rise of 2.3 K, whereas a former version of this model with fixed absolute humidity resulted only in a surface warming of 1.3 K for the same forcing (Manabe and Strickler, 1964). These were the first model manifestations of a potential water vapour feedback in a global warming scenario.

Lindzen (1990) criticised that the discussion of a potential climate warming due to CO_2 enhancement was focussed solely on the radiative mode of the cooling of the Earth surface. He argued that particularly in the tropics convective transport of latent heat into the middle troposphere would short-circuit the radiative resistance imposed by the bulk of the water vapour column in the lower troposphere and that therefore convection must be taken into account in an assessment of the water vapour feedback. The crucial question was whether convection enhances or diminishes UTH. Early attempts to check this consisted in measuring the vertical distribution of water vapour in regions of more or less convection (Inamdar and Ramanathan, 1994) or in cold and warm seasons (Rind et al., 1991). It turned out that convective regions are more humid than non-convective ones with a higher relative humidity over the entire tropospheric column (Inamdar and Ramanathan, 1994). Comparing summer vs. winter values of

ACPD
15, 29497–29521, 2015

middle and upper tropospheric humidity using satellite data showed that increased convection leads to increased water vapour above the 500 hpa level (Rind et al., 1991). Comparison of water vapour profiles above the tropical western and eastern Pacific regions led to the same conclusion, namely that increased convection does not lead to a drying of the upper troposphere (Rind et al., 1991). Studies using global circulation models (GCMs) showed that the specific humidity increases at all levels throughout the atmosphere in reaction to climate warming. Absolute (i.e. additive) changes are largest at the ground and decrease upwards in a more or less exponential manner. However, relative (i.e. multiplicative) changes are largest in the upper troposphere, and exceed there a factor of two (Mitchell and Ingram, 1992). Another GCM study showed that the feedback on global mean surface temperature changes, due to extratropical free tropospheric water vapour, exceeds the corresponding feedback of free tropospheric water vapour in the tropical zones by 50 % (Schneider et al., 1999). These findings motivate further studies of UTH changes in mid-latitude zones.

The old results obtained by Möller (1963) and Manabe and Wetherald (1967) led to the widely assumed view that the relative humidity, RH, will stay approximately unchanged in a warmer world (Ingram, 2002). While this might turn out true in a global mean sense, it is probably not true locally. A robust feature of climate models run under the assumption of surface warming is an increase of RH in the global upper troposphere above 200 hPa and at ±10° around the equator up to 500 hPa, a decrease in the subtropics and in the tropics between 500 and 200 hPa, and insignificant change of RH elsewhere (see e.g. Sherwood et al., 2010; Irvine and Shine, 2015, and references cited therein). This "elsewhere" includes in particular the free troposphere of the mid-latitudes, where we should thus expect small changes of RH at most. However, a recent comparison of decadal means of UTHi (UTH with respect to ice), for the decades 1980–1989 and 2000–2009, respectively, and performed for the 30 to 60 °N latitude belt, showed a moderate (few percent) but statistically significant increase of UTHi over large regions in this zone (Gierens et al., 2014). The data for this study had been obtained from 30 years of intercalibrated satellite data from the High-resolution

ACPD
15, 29497–29521, 2015

Infrared Radiation Sounder (HIRS) instruments on the NOAA polar orbiting satellite series (Shi and Bates, 2011). This finding was in accordance with previous studies detecting a moistening of the upper troposphere both globally and in the zonal mean (Soden et al., 2005). Those trends were based both on HIRS and Microwave Sounder Unit (MSU) data. It was later shown that the global mean upper tropospheric moistening could not be explained by natural sources and resulted primarily from an anthropogenic warming of the climate (Chung et al., 2014).

The apparent contradiction between an increasing UTH and a virtually constant RH in the midlatitudes inspired us to investigate how the upper-tropospheric humidity can change while the relative humidity is constant. It is possible to treat this question with analytical methods and radiative transfer calculations. This paper is only intended to demonstrate the principles and to give rough estimates.

Therefore, the main aim of our study is to understand if and how the UTH can change in cases where the RH will remain constant in a warming environment. As such, our methods are valid only over regions where RH remains constant. Our findings show that the UTH can still change under constant RH because of the weighting function that defines UTH. The weighting function can change because of changes in two quantities that define it, the peak emission altitude and the water vapour scale height. We describe the mechanisms with which the two properties of the weighting function can modify the UTH under the assumption of constant RH.

2 Analytical calculations

The upper tropospheric humidity, UTH, as obtainable from radiation measurements from nadir sounders as HIRS (Soden and Bretherton, 1993; Jackson and Bates, 2001) or the SEVIRI instrument on Meteosat (Schröder et al., 2014) is a weighted mean over a vertical profile of relative humidity, RH(z). There is some freedom in the choice of weighting function (also termed weighting kernel or Jacobian, see Jackson and Bates, 2001; Brogniez et al., 2009; Schröder et al., 2014). For the present purpose it suffices

ACPD
15, 29497–29521, 2015

to use a generic weighting function of the form (cf. Gierens et al., 2004)

$$K(z,\bar{z},H) = H^{-1} e^{-(z-\bar{z})/H} \exp\left[-e^{-(z-\bar{z})/H}\right], \tag{1}$$

where z is altitude, $\bar{z}$ is the altitude where the weighting function peaks (which is that altitude where the optical depth down from the top of the atmosphere reaches unity), and H is the scale height of an exponential water vapour profile. A derivation of this generic kernel function is given in the Appendix A. The shape of this function is illustrated in Fig. 1 for various choices of peak altitude and scale height.

The upper tropospheric humidity, UTH, is then given by the following integral:

$$\mathrm{UTH} = \int_0^\infty \mathrm{RH}(z) K(z,\bar{z},H)\,\mathrm{d}z. \tag{2}$$

If a profile RH(z) is fixed, UTH can still change whenever the scale height and/or the altitude of peak emission are changing.

2.1 Effect on scale height

Fixed relative humidity under warming implies that the actual water vapour pressure, e, and the saturation vapour pressure, e^*, change in the same proportion:

$$\mathrm{d}\ln e = \mathrm{d}\ln e^* = \frac{L}{R_\mathrm{w} T^2}\,\mathrm{d}T, \tag{3}$$

where R_w is the gas constant of water vapour.

There are two types of relative humidity at subzero temperatures, with respect to supercooled liquid water ($\mathrm{RH_w}$) and with respect to ice ($\mathrm{RH_i}$). In the equation above we have correspondingly two possibilities for the latent heat, L, which can be latent heat of evaporation ($L_\mathrm{w} = 2.50\,\mathrm{MJ\,kg^{-1}}$) or sublimation ($L_\mathrm{w} = 2.84\,\mathrm{MJ\,kg^{-1}}$). Obviously, vapour

ACPD
15, 29497–29521, 2015

pressure can change in proportion to the saturation vapour pressure only for one of these versions. If $RH_i(z)$ is constant, then $RH_w(z)$ would change on warming, and vice versa. Thus, only one version of relative humidity can be constant under warming conditions (which might be a little surprise, because this has never been explicitly stated to the authors' knowledge, see the Appendix B). The following derivation is valid for both forms of the Clausius–Clapeyron equation, thus we will not show an index "i" or "w".

The vapour pressure scale height is defined as

$$H = -\left(\frac{\mathrm{d}\ln e}{\mathrm{d}z}\right)^{-1}. \tag{4}$$

This means

$$\begin{aligned} -\frac{\mathrm{d}H^{-1}}{\mathrm{d}t} &= \frac{\mathrm{d}}{\mathrm{d}t}\left(\frac{\mathrm{d}\ln e}{\mathrm{d}z}\right) \\ &= \frac{\mathrm{d}}{\mathrm{d}z}\left(\frac{\mathrm{d}\ln e}{\mathrm{d}t}\right) \\ &= \frac{\mathrm{d}}{\mathrm{d}z}\left(\frac{L}{R_w T^2}\cdot\frac{\mathrm{d}T}{\mathrm{d}t}\right) \\ &= \frac{L}{R_w}\left[\frac{\mathrm{d}}{\mathrm{d}z}\left(\frac{1}{T^2}\right)\cdot\frac{\mathrm{d}T}{\mathrm{d}t} + \frac{1}{T^2}\cdot\frac{\mathrm{d}^2T}{\mathrm{d}z\,\mathrm{d}t}\right] \\ &= \frac{L}{R_w}\left[-\frac{2}{T^3}\frac{\mathrm{d}T}{\mathrm{d}z}\cdot\frac{\mathrm{d}T}{\mathrm{d}t} + \frac{1}{T^2}\cdot\frac{\mathrm{d}^2T}{\mathrm{d}z\,\mathrm{d}t}\right] \\ &= \frac{L}{R_w T^2}\left[\frac{\mathrm{d}^2T}{\mathrm{d}z\,\mathrm{d}t} - \frac{2}{T}\frac{\mathrm{d}T}{\mathrm{d}z}\cdot\frac{\mathrm{d}T}{\mathrm{d}t}\right]. \end{aligned} \tag{5, 6}$$

Now we set

$$\Delta T = (\mathrm{d}T/\mathrm{d}t)\Delta t,$$

ACPD
15, 29497–29521, 2015

and compute the corresponding ΔH^{-1} as follows:

$$\Delta H^{-1} = -\frac{L}{R_w T^2}\left[\frac{\mathrm{d}}{\mathrm{d}z}(\Delta T) - \frac{2}{T}\Gamma \Delta T\right]. \quad (7)$$

$\Gamma = \mathrm{d}T/\mathrm{d}z$ is the temperature lapse rate, ΔT is the temperature change in a certain altitude, and $\mathrm{d}\Delta T/\mathrm{d}z$ is the "lapse rate" of this warming tendency.

Let us make a few estimates: first, $L/R_w T^2 \approx 0.1\,\mathrm{K}^{-1}$. Then say, $\Delta T/T \approx 0.01$ and $\Gamma \approx -0.01\,\mathrm{K\,m}^{-1}$. Then the second right-hand side (rhs) term times prefactor is of the order $-10^{-5}\,\mathrm{m}^{-1}$. The first rhs term is either zero, if the temperature would change equally in all altitudes, or we can assume that it changes in proportion to the actual temperature (i.e. $\Delta T(z) \propto T(z)$ with a proportionality factor of about -0.01 to be consistent with the previous assumptions) and thus it would be proportional to the lapse rate. Thus the first factor is assumed to range between zero and half of magnitude as the second term. That is we estimate $\Delta H^{-1} \approx -10^{-5}\,\mathrm{m}^{-1}$. Now

$$\mathrm{d}H = -\mathrm{d}H^{-1} \cdot H^2. \quad (8)$$

H itself is of the order 2 km, thus we have $\Delta H \approx 40$ m. The scale height of water vapour in the tropopause can thus be expected to increase by a few ten metres as a consequence of tropospheric warming, even if the profile of relative humidity should be unchanged.

To corroborate these estimates we have analysed the changes in the scale height of water vapour (ΔH) using observed air temperatures (T) and observed changes (ΔT) in the past 30 years. The data of T and ΔT were provided by the study of Zerefos et al. (2014) and refer to the period 1980 to 2011. Trend estimates were calculated from NCEP reanalysis data after filtering out natural variations such as the QBO and the 11 year solar cycle, and excluding periods following major volcanic eruptions. The trends were derived for various latitude zones and atmospheric layers. In our analysis we have used the observed temperature trends as input to Eq. (7) to estimate the

ACPD
15, 29497–29521, 2015

changes in scale height from 1980 to 2011 in the northern high latitudes (60–90 °N), the mid-latitudes (30–60 °N) and the tropics (5–30 °N), for the atmospheric layers of 1000–925, 925–500, and 500–300 hPa. The trends were given per decade so we multiplied the results by 3 to calculate the overall change in the past 30 years (ΔT). Table 1 summarises the observed temperature changes taken from the study by Zerefos et al. (2014), as well as the calculated changes in scale height of water vapour at the three mentioned latitudinal belts. The ΔH calculations were done using Eqs. (7) and (8). In Eq. (7) we considered a fixed temperature lapse rate (Γ) of $-0.01\,\mathrm{K\,m^{-1}}$ and different ratios L/RT^2 for each layer. L_w, the enthalpy of evaporation, has been used for the layers of 1000–925 and 925–500 hPa, and L_i, the enthalpy of sublimation, has been used for the layer of 500–300 hPa. The range given for ΔH corresponds to the two assumptions of (i) ΔT constant over the layers and (ii) ΔT proportional to T over the layers (as above). In Eq. (8) we considered a fixed water vapour scale height (H) of 2 km to derive the final ΔH in metres.

From Table 1 it appears that the observed changes in ΔH during the past 30 years were generally small. The largest changes in the scale height of upper tropospheric humidity (layer 500–300 hPa) were calculated for the high latitudes, where ΔH increased by 15 to 30 m. The respective changes in the middle latitudes and the tropics were estimated to be 7.8–15.6 and 4.5–9 m, respectively. The changes in scale height were larger in the lower troposphere than in the upper troposphere. This can be explained by the fact that the ratio $\Delta T/T$ which is proportional to ΔH, was larger in the lower atmospheric layers than at 300–500 hPa (see Table 1), and therefore the ΔH was larger as well. From the analysis it appears that the high latitudes will probably be the most vulnerable to UTH changes in a warming climate. However, our calculations, which were based on observed changes of layer-mean air temperatures, give us a good indication as to the extent of the changes in the water vapour scale height that can occur in the atmosphere. These are very small indeed; it would be very difficult to compute them directly from data sets of humidity profiles with sufficient precision.

ACPD
15, 29497–29521, 2015

2.2 Effect on peak emission altitude

In this section we show calculations of how the peak emission altitude (where the optical depth reaches unity) changes with changing temperature but fixed relative humidity. This change is generally different for each spectral line, thus it is a function of wavenumber (or wavelength).

For the calculation we use SBDART (Santa Barbara DISORT Atmospheric Radiative Transfer, Ricchiazzi et al., 1998). This code is based on a LOWTRAN 7 transmission model, having a spectral resolution of 20 cm^{-1}, which suffices for the present purpose. We chose the wavelength range 4.6 to 10 µm and used the spectral resolution of LOWTRAN, 20 cm^{-1}. This wavelength range contains in particular the strong water vapour vibration-rotation band at about 6.3 µm, which is the basis for determining UTH (e.g. channel 12 of HIRS). With this setting we performed three model runs for a cloud-free mid-latitude summer atmosphere, one with the standard profiles of temperature and water vapour concentration (from the 1976 compilation of standard atmospheres by Mc Clatchey), and two that have increased temperature by 0.5 and 1 K, respectively, up to 12 km altitude and correspondingly increased water vapour concentration, such that the relative humidity is the same as before. For the transition between water vapour concentration and relative humidity we use SBDART's function relhum. From the output of the model runs we then take the optical depth in each wavelength interval τ_λ and search by linear interpolation that altitude, $\overline{z}(\lambda)$ where $\tau_\lambda = 1$. Figure 2 shows the results. The left panel shows the peak emission altitude for the standard midsummer atmosphere, while the right panel shows how the emission altitude increases when the temperature throughout the tropopause increases by 0.5 and 1 K. There are certain narrow bands for which SBDART computes a surprisingly strong increase of $\overline{z}$, amounting to several 100 m. Over most of the vibration-rotation band, $\overline{z}$ increases by about 30 to 70 m.

An independent analytical estimate of $\Delta\overline{z}$ can be performed using equations in Stephens et al. (1996, Sect. 5a; in the following we use their nomenclature). Their

ACPD
15, 29497–29521, 2015

Eq. (15) shows that the optical depth at the level where the temperature is 240 K increases by 5 % when the temperature increases by 1 K. The reason for this is the corresponding increase of the airmass factor (water vapour above that level) by approximately 10 % (Eqs. 12 and 8), that is, from u_0 to $1.1u_0$. Calculating the vertical distance from the 240 K level to that level where the airmass is 10 % lower should be an appropriate estimate for $\Delta\overline{z}$ (even if $\overline{z}$ is not generally at the 240 K level). For this purpose, we combine Eqs. (11) and (12) of Stephens et al. (1996), use the hydrostatic equation to transform the vertical coordinate from pressure to altitude, use the gas equation to get rid of the density, and arrive at:

$$\Delta\overline{z} \approx \frac{\Delta u}{u_0}\frac{T_0 R_a}{e^{\lambda\beta} g} \approx 68\,\mathrm{m}, \tag{9}$$

with the gas constant of air, $R_a = 287\,\mathrm{J\,(kg\,K)^{-1}}$, the gravitational acceleration, $g = 9.81\,\mathrm{m\,s^{-2}}$, $\Delta u/u_0 \approx 0.1$, and the constants $\lambda = 23.1, \beta = 0.1$ from Stephens et al. (1996, the latter can be found in Eq. 22). Thus this simple analytical estimate confirms the result from the radiative transfer simulation, viz. that the peak emission level rises as a consequence of climate warming by about $70\,\mathrm{m\,K^{-1}}$ of temperature increase.

3 Results and discussion

3.1 Impacts on the kernel function

The changes in scale height and peak emission altitude lead to a change of the factor $(z - \overline{z})/H$ in the kernel function; it increases in a warming climate. The corresponding absolute and relative changes of the kernel function are shown in Fig. 3 for an assumed increase of $\overline{z}$ from 7.0 to 7.05 km and a small increase of H from 2.00 to 2.01 km.

The curves show that weights below 7 km get reduced and weights above 7 km increased. The colder layers thus gain in weight, while the warmer ones loose importance. It is in particular noteworthy that not only the immediate neighbourhood of the

ACPD
15, 29497–29521, 2015

old or new $\overline{z}$ is affected by such a change; instead, the kernel function is modified everywhere. Far below or above $\overline{z}$ these changes are negligible because the original values were negligible anyway. But closer to $\overline{z}$ – yet not only in the immediate neighbourhood – these changes are significant; they lead to modification of the retrieved UTH values even if the relative humidity profiles do not change at all. How large these changes are, will now be tested with real radiosonde data.

3.2 Application to real profiles

In this section we examine the effects of the changes in the kernel function on the UTH field using real humidity profiles from radiosondes. We wanted to investigate how UTH changes when both quantities of the weighting function change according to our previous calculations. We assume again an increase in $\overline{z}$ from 7.00 to 7.05 km and an increase in H from 2.00 to 2.01 km. We have analysed all the humidity profiles for the period February 2000 to April 2001 as obtained from the Lindenberg corrected RS80A routine radiosondes. Measurements were performed 4 times per day corresponding roughly to times 00:00, 06:00, 12:00 and 18:00 UTC. Each radiosonde profile provides information on the pressure, temperature and relative humidity with respect to liquid water per height. In total we analysed 1564 available humidity profiles. Details on the radiosonde data can be found in the study by Spichtinger et al. (2003).

The radiosondes provide relative humidity profiles with respect to water. A conversion to relative humidity profiles with respect to ice is only possible at sub-zero temperatures. Since our radiosonde profiles contain temperature above 0 °C, we illustrate the impact of kernel-function changes on UTH for UTH with respect to liquid water.

In our analysis we used two weighting functions; one weighting function with standard peak emission altitude and standard scale height (7.00 and 2.00 km, respectively), and a second weighting function with increased peak emission altitude and increased scale height (7.05 and 2.01 km, accordingly). Each weighting function was multiplied with the profiles of RH from the surface up to the lower stratosphere (≈ 16 km). The UTH was calculated from the integral as given in Eq. (2), using a trapezoidal rule.

ACPD
15, 29497–29521, 2015

Since our target was to estimate the impact on UTH from different weighting functions, we estimated for each profile two values of UTH; one value using the first weighting function and another value using the second weighting function. We then estimated the differences in UTH per profile to see the results.

The right panel of Fig. 4 shows the differences in UTH resulting from the change in the two quantities of the weighting function i.e. of $\overline{z}$ by 0.05 km and of H by 0.01 km. The results indicate small differences in UTH between 0.3 and −1.2 %. Mean differences were the order of −0.2 % with standard deviation of differences of about 0.2 %. Evidently it can be inferred that a change in the properties of the weighting function, i.e. $\Delta\overline{z} = 0.05$ km and $\Delta H = 0.01$ km, can result in small changes in UTHi of not more than roughly ±1 %.

Before closing this paragraph, noteworthy discussing is the left panel of Fig. 4, which shows two individual profiles of RH over Lindenberg (blue and magenta) along with the changes in the integrands of Eq. (2) (red and green). The blue line shows the profile of RH for 15 July 2000 taken at 00:00 UT while the line with purple colour shows the respective profile for 18 July 2000. We note here that these specific profiles resulted in UTH differences with opposite sign, e.g. negative difference in UTH from the profile of 15 July and positive difference from the profile of 18 July. Comparing the two individual profiles in general, we can clearly see that the first profile had higher RH than the second profile up to 7.5 km height, lower RH between 7.5 and 8 km height, higher RH up to 10 km and much lower RH above 10 km height. Furthermore, the very dry layer between 2 and 3 km altitude on 18 July is noteworthy.

As stated above, the change in the kernel functions give the lower layers less, the upper layers more weight. This means for the present examples that the very dry layer in the lower troposphere on 18 July gets reduced in weight, and instead the moist layer between 10 and 12 km gains weight. The result of this is an increase of UTH for the 18 July. For 15 July, in turn, the main effect is the gain in weight of the strong humidity decrease at 10 km altitude which results in a decrease of UTH.

ACPD
15, 29497–29521, 2015

We see that the change in UTH depends not only on "climatological" changes of scale height and peak emission altitude. For an individual profile of relative humidity it depends strongly on the shape of that profile. We have seen mostly negative changes at Lindenberg, but at other locations the conditions may be different such that positive changes would prevail. This could be studied with other sets of radiosonde data, but is not in the scope of this paper which shows the principles only. Whether positive or negative changes prevail depends also strongly on the choice of an appropriate $\overline{z}$, that is, it depends on the filter function of the instrument detecting the upper tropospheric water vapour. A high peak emission altitude (say 9 km or so) would already mean that much dry stratospheric air is seen and after an increase of $\overline{z}$ this would even more be the case, such that UTH would decrease mostly. A more neutral partition of signs of UTH changes is only possible if $\overline{z}$ is located in the middle troposphere. Anyhow, the UTH changes under the condition of constant relative humidity are small, which implies that their detection with statistical significance needs very long homogeneous time series.

4 Summary and outlook

In this paper we treated the question how the upper-tropospheric humidity (UTH) can change in regions where relative humidity will only marginally change as a consequence of tropospheric warming. This is possible since UTH is a weighted mean over the profile of relative humidity. This mean can change once the weights change even when the RH(z) profile stays constant.

Two quantities in the weighting function can change: the scale height of the water vapour concentration profile, and the peak emission altitude (which varies with wavelength). We showed that the change of the water vapour concentration scale height is rather small, of the order 10 m, with latitudinal and vertical variations. In the midlatitude upper troposphere it might have been increased by 10 m between 1980 and 2010, which is a relative change of less than 1 %.

ACPD
15, 29497–29521, 2015

The peak emission altitudes in the 6.3 µm band of water vapour generally increases by around 30 to 70 m for a temperature increase throughout the troposphere of 0.5 to 1 K. It seems that there are a few narrow spectral lines that react much stronger than the majority of the band, where the peak emission altitude even increases by several 100 metres. But an analytical calculation using empirical formulae provided by Stephens et al. (1996) led to a similar increase of about 70 m for the whole band.

We applied the computed changes of the kernel function to 14 months of real radiosonde profiles of relative humidity and found that mostly the resulting UTH is smaller than before after increases of scale height and peak emission altitude. The absolute changes of UTH due to changes in the kernel functions are however very small, typically smaller than 1 %. Such changes would hardly be detectable even in long humidity time series. The detection of larger changes, in turn, implies that the condition assumed in this paper, that is, constant relative humidity, is violated, that is, absolute UTH changes of more than one percent or so point to systematic (climatological) changes in relative humidity.

Determining decadal changes (2000–2009 vs. 1980–1989) of UTHi for the northern midlatitudes, 30–60 °N, from intercalibrated HIRS data (Gierens et al., 2014) resulted in statistically highly significant increases of more than 2 % in a large fraction of this latitude belt. As we see from the present analyses, such an increase would be unexpected under the assumption that the relative humidity would have stayed nearly constant during these 30 years, both for the size of the effect (exceeding 1 %) and its main direction (positive). Based on the observed increase of UTHi we may thus conclude that the relative humidity itself must have increased as well between 1980 and 2009 in large parts of the northern midlatitudes.

ACPD
15, 29497–29521, 2015

Appendix A: Derivation of the generic kernel function

The kernel function is defined in radiative transfer as

$$K(z) = \mathrm{d}\mathcal{T}(z)/\mathrm{d}z = \chi(z)\mathcal{T}(z),$$

where $\mathcal{T}(z)$ is the transmission from altitude z to space and where $\chi(z)$ is the local extinction coefficient. The latter is proportional to the local concentration of water vapour. Assuming an exponential water vapour profile in the troposphere with scale height H we can set

$$\chi(z) = c\rho_0 \exp(-z/H),$$

where ρ_0 is the vapour partial density at ground. For the transmission function we have:

$$\mathcal{T}(z) = \exp(-\int_z^\infty \chi(z')\mathrm{d}z').$$

Inserting the expression for $\chi(z)$ and performing the integration yields

$$\mathcal{T}(z) = c\rho_0 \exp(-z/H) \exp[-Hc\rho_0 e^{(-z/H)}].$$

Now we define $\bar{z}$ as

$$e^{\bar{z}/H} = Hc\rho_0$$

and find the expression for the kernel function that is used in the paper. Note, that the small difference (a few percent) between density and pressure scale heights has been considered dispensable for order-of-magnitude estimates and has thus been ignored.

ACPD
15, 29497–29521, 2015

The meaning of $\overline{z}$ is easy to find. The optical depth, τ, at $\overline{z}$ is unity:

$$\tau(\overline{z}) = \int_{\overline{z}}^{\infty} \chi(z)\mathrm{d}z \tag{A1}$$

$$= c\rho_0 \int_{\overline{z}}^{\infty} e^{-z/H}$$

$$= Hc\rho_0 e^{-\overline{z}/H} = 1. \tag{A2}$$

Appendix B: Only one kind of relative humidity can be constant

Dividing the two versions of the Clausius–Clapeyron equation, we have

$$\frac{\mathrm{d}\ln e_{\mathrm{i}}^*}{\mathrm{d}\ln e_{\mathrm{w}}^*} = \frac{L_{\mathrm{i}}}{L_{\mathrm{w}}} =: \kappa.$$

Assuming that the relative humidity with respect to ice is constant, we then have

$$\mathrm{d}\ln e = \mathrm{d}\ln e_{\mathrm{i}}^*,$$

but

$$\mathrm{d}\ln e = \kappa \mathrm{d}\ln e_{\mathrm{w}}^*.$$

Integrating this differential equation yields

$$\frac{e(t)}{e(0)} = \left(\frac{e_{\mathrm{w}}^*(t)}{e_{\mathrm{w}}^*(0)}\right)^{\kappa},$$

ACPD
15, 29497–29521, 2015

which means that then vapour pressure and saturation vapour pressure with respect to supercooled liquid water change in different proportions as $\kappa \neq 1$.

Vice versa, that is, if the relative humidity with respect to liquid water is constant, we arrive at

$$\frac{e(t)}{e(0)} = \left(\frac{e_i^*(t)}{e_i^*(0)} \right)^{1/\kappa} .$$

This is rather trivial, but has to our knowledge never been stated explicitely.

Acknowledgements. The article processing charges for this open-access publication were covered by a Research Centre of the Helmholtz Association.

References

Brogniez, H., Roca, R., and Picon, L.: A study of the free tropospheric humidity interannual variability using Meteosot data and an advection–condensation transport model, J. Climate, 22, 6773–6787, 2009. 29501

Chung, E.-S., Soden, B., Sohn, B., and Shi, L.: Upper-tropospheric moistening in response to anthropogenic warming, P. Natl. Acad. Sci. USA, 111, 11636–11641, 2014. 29501

Clough, S., Iacono, M., and Moncet, J.-L.: Line-by-line calculations of atmospheric fluxes and cooling rates: application to water vapor, J. Geophys. Res., 97, 15761–15785, 1992. 29499

Gierens, K., Kohlhepp, R., Spichtinger, P., and Schroedter-Homscheidt, M.: Ice supersaturation as seen from TOVS, Atmos. Chem. Phys., 4, 539–547, doi:10.5194/acp-4-539-2004, 2004. 29502

Gierens, K., Eleftheratos, K., and Shi, L.: Technical Note: 30 years of HIRS data of upper tropospheric humidity, Atmos. Chem. Phys., 14, 7533–7541, doi:10.5194/acp-14-7533-2014, 2014. 29500, 29511

Inamdar, A. and Ramanathan, V.: Physics of greenhouse effect and convection in warm oceans, J. Climate, 7, 715–731, 1994. 29499

Ingram, W.: On the robustness of the water vapor feedback: GCM vertical resolution and formulation, J. Climate, 15, 917–921, 2002. 29500

ACPD
15, 29497–29521, 2015

Irvine, E. A. and Shine, K. P.: Ice-supersaturation and the potential for contrail formation in a changing climate, Earth Syst. Dynam. Discuss., 6, 317–349, doi:10.5194/esdd-6-317-2015, 2015. 29500

Jackson, D. and Bates, J.: Upper tropospheric humidity algorithm assessment, J. Geophys. Res., 106, 32259–32270, 2001. 29501

Kiemle, C., Schäfler, A., and Voigt, C.: Detection and analysis of water vapour transport, in: Atmospheric Physics. Background – Methods – Trends, edited by: Schumann, U., chap. 11, 169–184, Springer, Heidelberg, Germany, 2012. 29498

Lindzen, R.: Some coolness concerning global warming, B. Am. Meteorol. Soc., 71, 288–299, 1990. 29499

Manabe, S. and Strickler, R.: Thermal equilibrium of the atmosphere with a convective adjustment, J. Atmos. Sci., 21, 361–385, 1964. 29499

Manabe, S. and Wetherald, R.: Thermal equilibrium of the atmosphere with a given distribution of relative humidity, J. Atmos. Sci., 24, 241–259, 1967. 29499, 29500

Mitchell, J. and Ingram, W.: Carbon dioxide and climate: mechanisms of changes in cloud, J. Climate, 5, 5–21, 1992. 29500

Möller, F.: On the influence of changes in the CO_2 concentration in air on the radiation balance of the earth's surface and on climate, J. Geophys. Res., 68, 3877–3886, 1963. 29499, 29500

Ricchiazzi, P., Yang, S., Gauthier, C., and Sowle, D.: SBDART: a research and teaching software tool for plane-parallel radiative transfer in the Earth's atmosphere, B. Am. Meteorol. Soc., 79, 2101–2114, 1998. 29506

Rind, D., Chiou, E., Chu, W., Larsen, J., Oltmans, S., Lerner, J., McCormick, M., and McMaster, L.: Positive water vapour feedback in climate models confirmed by satellite data, Nature, 349, 500–503, 1991. 29499, 29500

Schneider, E., Kirtman, B., and Lindzen, R.: Tropospheric water vapor and climate sensitivity, J. Atmos. Sci., 56, 1649–1658, 1999. 29500

Schröder, M., Roca, R., Picon, L., Kniffka, A., and Brogniez, H.: Climatology of free-tropospheric humidity: extension into the SEVIRI era, evaluation and exemplary analysis, Atmos. Chem. Phys., 14, 11129–11148, doi:10.5194/acp-14-11129-2014, 2014. 29501

Sherwood, S., Roca, R., Weckwerth, T., and Andronova, N.: Tropospheric water vapor, convection, and climate, Rev. Geophys., 48, RG2001, doi:10.1029/2009RG000301, 2010. 29500

ACPD
15, 29497–29521, 2015

Shi, L. and Bates, J.: Three decades of intersatellite-calibrated High-Resolution Infrared Radiation Sounder upper tropospheric water vapor, J. Geophys. Res., 116, D04108, doi:10.1029/2010JD014847, 2011. 29501

Soden, B. and Bretherton, F.: Upper tropospheric relative humidity from the GOES 6.7 µm channel: method and climatology for July 1987, J. Geophys. Res., 98, 16669–16688, 1993. 29501

Soden, B., Jackson, D., Ramaswamy, V., Schwarzkopf, M., and Huang, X.: The radiative signature of upper tropospheric moistening, Science, 310, 841–844, 2005. 29501

Spichtinger, P., Gierens, K., Leiterer, U., and Dier, H.: Ice supersaturation in the tropopause region over Lindenberg, Germany, Meteorol. Z., 12, 143–156, 2003. 29508

Stephens, G., Jackson, D., and Wittmeyer, I.: Global observations of upper-tropospheric water vapor derived from TOVS radiance data, J. Climate, 9, 305–326, 1996. 29506, 29507, 29511

Zerefos, C. S., Tourpali, K., Zanis, P., Eleftheratos, K., Repapis, C., Goodman, A., Wuebbles, D., Isaksen, I. S. A., and Luterbacher, J.: Evidence for an earlier greenhouse cooling effect in the stratosphere before 1980 over the Northern Hemisphere, Atmos. Chem. Phys., 14, 7705–7720, doi:10.5194/acp-14-7705-2014, 2014. 29504, 29505, 29517

ACPD
15, 29497–29521, 2015

Table 1. Layer-mean air temperatures (T), changes in air temperatures (ΔT over 30 years), ratios ($\Delta T/T$) and changes in scale height of water vapour (ΔH) at three latitudinal belts: 60–90, 30–60 and 5–30 °N. The data of T and ΔT were provided by the study of Zerefos et al. (2014) and refer to the period 1980 to 2011. The ΔT were calculated from NCEP reanalysis and filtered from natural variations.

	60–90 °N			
Layer	ΔT (K)	T (K)	$\Delta T/T$	ΔH (m)
1000–925 hPa	2.52	265.0	0.00951	29.3–58.6
925–500 hPa	0.87	255.9	0.00340	11.3–22.6
500–300 hPa	0.75	230.8	0.00325	15.0–30.0
	30–60 °N			
Layer	ΔT (K)	T (K)	$\Delta T/T$	ΔH (m)
1000–925 hPa	0.84	282.6	0.00297	8.1–16.2
925–500 hPa	0.78	269.9	0.00289	8.8–17.2
500–300 hPa	0.45	241.4	0.00186	7.8–15.6
	05–30 °N			
Layer	ΔT (K)	T (K)	$\Delta T/T$	ΔH (m)
1000–925 hPa	0.36	297.1	0.00121	3.0–6.0
925–500 hPa	0.51	282.7	0.00180	4.9–9.8
500–300 hPa	0.30	254.0	0.00118	4.5–9.0

ACPD
15, 29497–29521, 2015

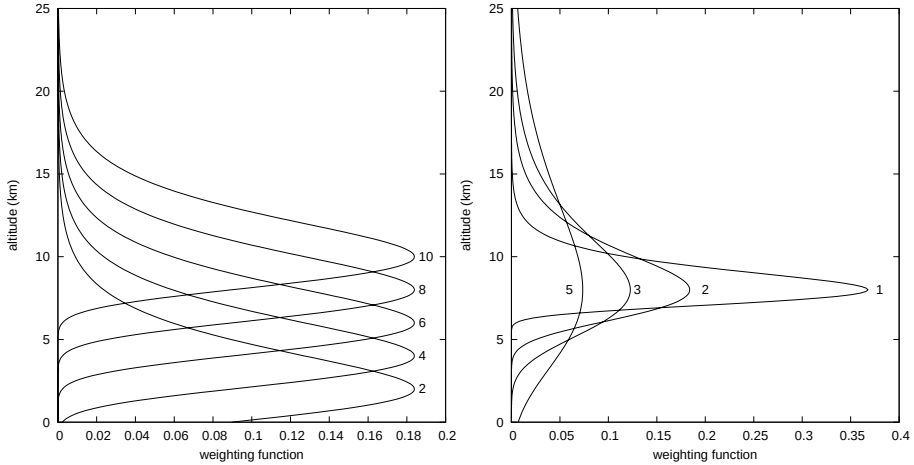

Figure 1. Generic weighting functions $K(z;\overline{z},H)$ for water vapour spectral transitions of various line strengths (parameter $\overline{z}$) and for various exponential vertical profiles of water vapour concentration (scale height H). The left panel **(a)** shows the dependence of $K(z)$ on $\overline{z}$ for a fixed scale height of 2 km. The labels at the curves are the corresponding values of $\overline{z}$ in km. Notice that the half widths of the weighting functions are almost independent of $\overline{z}$. The right panel **(b)** shows the dependence of $K(z)$ on the water vapour profile, i.e. on H. The numbers at the curves indicate the chosen value of H in km.

ACPD
15, 29497–29521, 2015

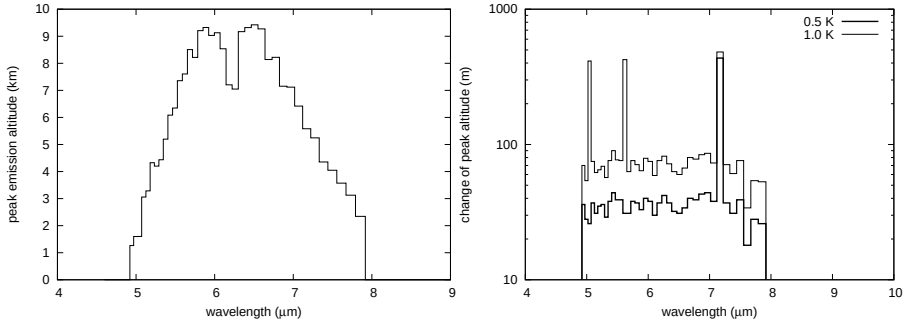

Figure 2. Left: peak altitude (in km) for infrared emission to space (i.e. altitude where the optical depth reaches unity) as a function of wavelength (in μm) in the spectral region of the strong ν_2 water vapour vibration-rotation band. The calculation has been done for a standard mid-latitude summer atmosphere. Right: change of the peak altitude (in metres) after a climate warming of 0.5 K (thick line) and 1 K (thin line) throughout the troposphere (up to 12 km) with constant relative humidity. The calculation has been performed for the mid-latitude summer atmosphere and the same wavelength region as in the left panel.

ACPD
15, 29497–29521, 2015

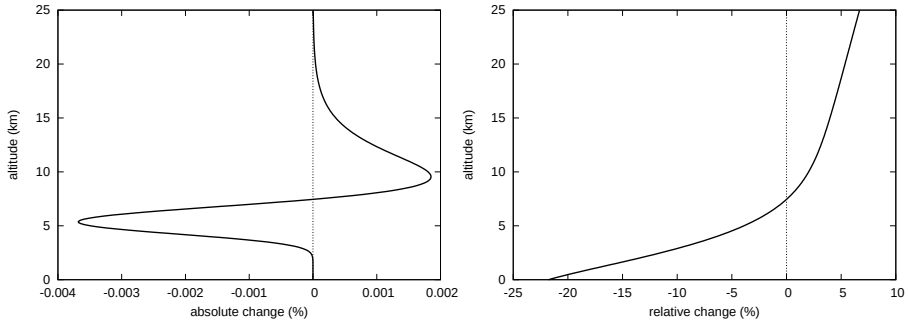

Figure 3. Absolute (left) and relative (right) change of altitude dependent weights in the kernel function (Eq. 1) after an increase of $\overline{z}$ from 7.00 to 7.05 km and a small increase of H from 2.00 to 2.01 km.

ACPD
15, 29497–29521, 2015

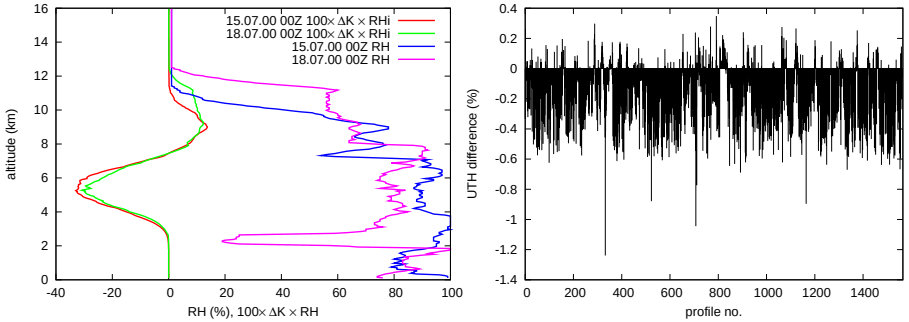

Figure 4. Left: profiles of relative humidity (with respect to water) measured with radiosondes launched at Lindenberg/Germany on 15 July 2000, 00:00 UTC (blue), and 18 July 2000, 00:00 UTC (magenta); these profiles have been multiplied with the difference of the two kernel functions of Fig. 3, resulting in the red profile for 15 July and the green profile for 18 July. Right: differences of UTH when the two kernel functions of Fig. 3 are applied to 1564 profiles of RH, measured from February 2000 to April 2001 with radiosondes launched at Lindenberg/Germany.

ACPD
15, 29497–29521, 2015